Hindawi
Advances in Materials Science and Engineering
Volume 2018, Article ID 7950607, 7 pages
https://doi.org/10.1155/2018/7950607

Research Article

Optimization of FCAW Parameters for Ferrite Content in 2205 DSS Welds Based on the Taguchi Design Method

Tianqi Li,[1] **Yingying Zhang**,[1] **Lei Gao**,[1] **and Yunhao Zhang**[2]

[1]*School of Mechanical Engineering, Liaoning Shihua University, Fushun 113001, Liaoning, China*
[2]*School of Aeronautical Manufacturing Engineering, Nanchang Hangkong University, Nanchang 330000, Jiangxi, China*

Correspondence should be addressed to Yingying Zhang; zyy_fs@163.com

Received 27 September 2018; Revised 1 December 2018; Accepted 11 December 2018; Published 27 December 2018

Guest Editor: Mohamed Abdel-Hady Gepreel

Copyright © 2018 Tianqi Li et al. This is an open access article distributed under the Creative Commons Attribution License, which permits unrestricted use, distribution, and reproduction in any medium, provided the original work is properly cited.

This study presents the Taguchi design method with L9 orthogonal array which was carried out to optimize the flux-cored arc welding (FCAW) process parameters such as welding current, welding voltage, welding speed, and torch angle with reference to vertical for the ferrite content of duplex stainless steel (DSS, UNS S32205) welds. The analysis of variance (ANOVA) was applied, and a mathematical model was developed to predict the effect of process parameters on the responses. The results indicate that welding current, welding voltage, welding speed, torch angle with reference to vertical, and the interaction of welding voltage and welding speed are the significant model terms connected with the ferrite content. The ferrite content increases with the increase of welding speed and torch angle with reference to vertical, but decreases with the increase of welding current and welding voltage. Through the developed mathematical model, the target of 50% ferrite content in weld metal can be obtained when all the welding parameters are set at the optimum values. Finally, in order to validate experimental results, confirmation tests were implemented at optimum working conditions. Under these conditions, there was good accordance between the predicted and the experimental results for the ferrite content.

1. Introduction

Duplex stainless steel (DSS) typically contains the microstructures consisting of almost equal proportions of ferrite and austenite phases. The fine ferrite-austenite microstructure of these materials promotes a good combination of anticorrosion and mechanical properties [1–3]. Duplex stainless steel is a common engineering material used in oil refining, food processing, wastewater treatment, and pharmaceuticals as well.

The increased use of duplex stainless steels in industrial applications will demand a better understanding of those weld parameters that affect weldability. Most of the welding processes, such as laser beam welding (LBW), shielded metal arc welding (SMAW), tungsten inert gas (TIG) welding, and submerged arc welding (SAW), can be used for welding duplex stainless steels [4–6]. Flux-cored arc welding (FCAW) process is also one of the most popular technologies for duplex stainless in manufacturing industries because it produces better and more consistent mechanical properties and higher deposition rates. However, a major problem is that the thermal cycle can degrade the strength and corrosion resistance of weld metal by producing unbalanced ferrite/austenite content, and any attempt to increase heat input changes the welding parameters, probably leading to precipitation of the secondary phase such as σ phase which also reduces the corrosion resistance and strength of weld [1, 7]. Therefore, the studies that control the ferrite/austenite phase ratio of weld metal are necessary. Welding process parameters are important factors that establish the approximately equal proportion of the ferrite/austenite phase (1 : 1) in the weld metal area. Usually, the appropriate ferrite content is 40–60% for good performance of the dual-phase steel to satisfy the requirement for which it is expected in the weld joint.

The relationship between the welding process parameters and the ferrite content can be modeled by using mathematical means. Mathematical models can be used to

understand the effect of welding process parameters on the ferrite content variables. The Taguchi method (TM) was a robust design method, originally developed to improve the quality of manufactured goods by Genichi Taguchi, and was effectively used in the optimization of multiple objectives by gray relational analysis [8–10]. The Taguchi method provides the research staff with a scientific and efficient way for ascertaining nearly optimal design parameters.

Though the study using Taguchi methods on weld geometries and mechanical properties has always been reported in literatures [11–14], it appears that the optimization of FCAW process parameters for the ferrite content in duplex stainless steel using the Taguchi method has hardly been studied. In view of the abovementioned facts, the Taguchi method with L9 orthogonal array and ANOVA is employed to analyze the effect of each weld processing parameter (welding current, welding voltage, welding speed, and torch angle with reference to vertical) for the ferrite content in flux-cored weld metal of 2205 DSS. The final intent of this research is to optimize the FCAW process parameters using the developed model to ensure that the ferrite content is close to 50% in 2205 DSS welds.

2. Experimental Work

The experiments were implemented by using a set of programmable welding equipment. The material chosen for the study was 12 mm DSS boards corresponding to UNS S32205, whose chemical composition is given in Table 1. Also, the chemical composition of filler metal (ER 2209, 1.2 mm diameter) is listed in Table 1. The welding joints were designed into a single V groove with an angle of 60° and a blunt edge of 1 mm. The welding parameters are given in Table 2. The interpass temperature was 150°C. The mean ferrite content in weld metal was measured by the FERITSCOPE MP30. Metallographic sample preparation has been carried out by grinding and polishing. To characterize the microstructures, the samples were etched by using a solution of 1 g $K_2S_2O_5$, 30 ml HCl, and 80 ml H_2O. Microstructures were observed by using an optical microscope and a field emission scanning electron microscopy. The scanning electron microscope was operated at an accelerating voltage of 15 kV. The chemical composition of different phases was analyzed by using an energy dispersive spectrometer connected to a scanning electron microscope.

3. Results and Discussion

3.1. Construction of Design Matrix. The experimental data required to relate the FCAW process parameters with response were arranged by using the Taguchi L9 (3^4) orthogonal array with nine experimental runs. The results of process parameters and their corresponding average ferrite content of weld metal are presented in Table 3. Figure 1 shows the optical micrographs of the weld metal microstructures. The dark regions are ferrite while the bright regions are austenite. Obviously, the weld ferrite content of sample 3 is higher than that of sample 9.

3.2. Effect of Parameters on Ferrite Content. The analysis of variance (ANOVA) was performed for the ferrite content with a confidence interval of 95 percent, and a p value less than 0.05 was considered to be statistically significant [15–17]. The test for significance of the developed model and the test for significance on individual coefficients were performed by using Design-Expert software. By using the stepwise regression method, which removes the insignificant model items automatically, the ANOVA (Table 4) for the reduced quadratic model summarizes the analysis of the ferrite content variance of the response and shows the significant model items. The F-test named after Fisher [18] can be used to find out which welding process parameters have a significant effect on the ferrite content. Usually, the change of the welding process parameter has a significant influence on the ferrite content when the F value is large [19]. In addition, the table also reveals the adequacy measures R^2, predicted R^2, and adjusted R^2. The adequacy measures are very close to 1, which is appropriate and indicates the adequate model. "Adeq Precision" measures the signal-to-noise ratio, and the value greater than 4 is considered to be desirable [20].

In this study, from the analysis of variance, it is clear that the ferrite content model is significant. The table indicates that welding current, welding voltage, welding speed, torch angle with reference to vertical, and the interaction of welding voltage and welding speed are the significant model terms affecting the ferrite content, and the result also shows that the highest F value was obtained for the welding speed equal to 5003.32 in the model. The F value for the interaction of welding voltage and welding speed was equal to 76.58, which indicates that the interaction term has a relatively less effect on the model. The Adeq Precision value of 146.135 indicates an adequate signal and implies that the model can navigate the design space.

The ANOVA shows that there is a connection between the main effects of the four parameters. The final mathematical model for the ferrite content is determined by the following procedures and represented as follows:

(a) In terms of coded factors:

$$\text{ferrite content} = 42.14 - 5.24I - 3.72U + 4.8S + 1.82T + 0.92US. \quad (1)$$

(b) In terms of actual factors:

$$\text{ferrite content} = 107.41556 - 0.131I - 2.92556U - 0.56333S + 0.12111T + 0.076667US. \quad (2)$$

Further, the validity of the developed regression model was confirmed by constructing a scatter diagram. A typical scatter diagram for the ferrite content is shown in Figure 2. The scatter diagram reveals that there is a good correlation between the experimental and predicted values.

Figure 3 is a perturbation plot, which helps to compare the effect of all the factors at the center place in the design

Table 1: Compositions of 2205 DSS and ER 2209 (wt.%).

Element	C	Si	Mn	P	S	N	Mo	Ni	Cr	Cu
2205 DSS	0.195	0.520	0.829	0.026	0.002	0.156	3.23	5.70	22.09	0.229
ER 2209	0.032	0.601	0.666	0.012	0.004	0.137	4.29	7.95	22.59	0.202

Table 2: Process parameters and design levels used in experiments.

Parameters	Symbol	Units	Level 1	Level 2	Level 3
Welding current	I	Ampere	160	200	240
Welding voltage	U	Volt	20	23	26
Welding speed	S	cm/min	18	22	26
Torch angle with reference to vertical	T	Degree	0	15	30

Table 3: Design matrix with measured responses.

Trial no.	Process parameters				Response
	I (ampere)	U (volt)	S (cm/min)	T (degree)	Average ferrite content (%)
1	160	20	18	0	45.5
2	160	23	22	15	47.2
3	160	26	26	30	51.3
4	200	20	22	30	47.6
5	200	23	26	0	45.1
6	200	26	18	15	32.8
7	240	20	26	15	44.6
8	240	23	18	30	33.9
9	240	26	22	0	31.3

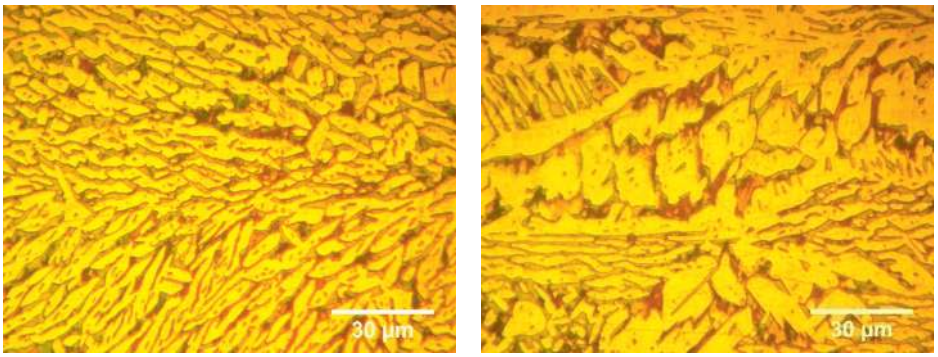

(a) (b)

Figure 1: Optical micrographs of weld metal microstructures of (a) sample 3 with the highest ferrite content and (b) sample 9 with the lowest ferrite content.

Table 4: ANOVA and R-square table for ferrite content reduced quadratic model.

Source	Sum of squares	DF	Mean square	F value	Prob > F	
Model	437.98	5	87.6	3170.36	<0.0001	Significant
I	102.97	1	102.97	3726.65	<0.0001	Significant
U	82.88	1	82.88	2999.74	<0.0001	Significant
S	138.24	1	138.24	5003.32	<0.0001	Significant
T	19.8	1	19.8	716.68	0.0001	Significant
US	2.12	1	2.12	76.58	0.0031	Significant
Residual	0.083	3	0.028			
Cor. total	438.06	8				
	R^2 = 0.9998				Pred R^2 = 0.9957	
	Adj. R^2 = 0.9995				Adeq Precision = 146.135	

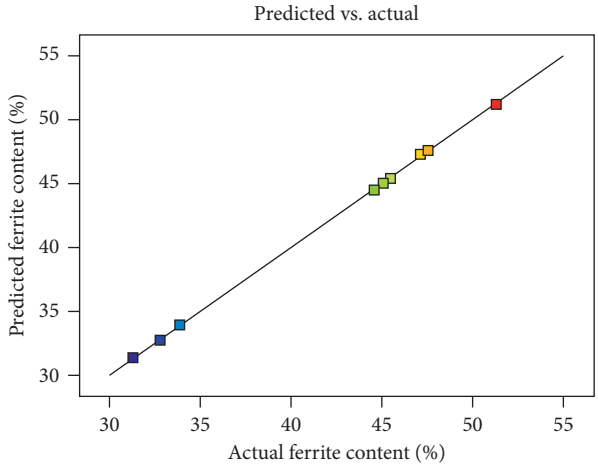

Figure 2: Predicted and experimental results of ferrite content.

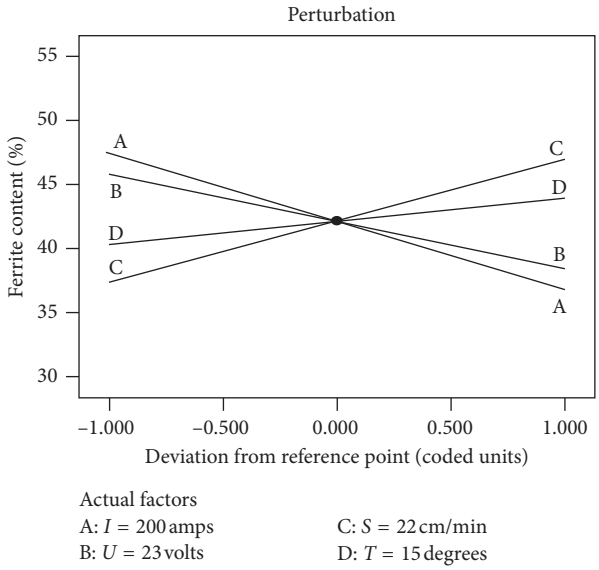

Figure 3: Perturbation plot showing the effect of all factors on the ferrite content.

space. It can be noticed that the ferrite content increases with the welding speed and torch angle with reference to vertical. This is because a higher welding speed reduces the heating time, and the electric arc becomes more decentralized from 0 degrees to 30 degrees for torch angle with reference to vertical. These two factors can cause lower heat input to the weld zone. Low heat input results in a fast cooling rate. There is no sufficient time for the diffusion of alloying elements (Cr, Ni, and Mo). The ferrite-to-austenite transformation ratio reduces during solidification [21]. From this figure, it is apparent that the welding current and the welding voltage have a negative effect on the ferrite content. It is due to the fact that heat input increases with welding current and welding voltage. There is sufficient time for the diffusion of alloying element under a slow cooling rate. Consequently, the ferrite-to-austenite transformation ratio increases under the effect of increased heat input, and a more austenite phase is generated during the process. In addition, σ phase precipitates in ferrite for a long time at high temperature, which further reduces the ferrite content. The SEM micrograph and EDS of the phases are shown in Figure 4. In contrast to the ferrite (α) and austenite (γ) phases, the light gray σ phase is richer in Cr.

4. Optimization of Results

In statistical software, the optimization part searches for a group of factor levels that simultaneously meet the goals placed on each of the factors and responses by using the developed mathematical model in the design space. The goals are combined into an overall desirability function. As displayed in Table 5, the optimization criterion has been executed for 2205 DSS welds. In the criterion, the process parameters are kept within the scope of the stationary design space. The goal response was set to the target of 50% ferrite content. However, the ferrite-austenite phase balance (1 : 1) imparts very desirable properties to the material [22–24]. The optimal results are listed in Table 6 with their desirability.

5. Confirmation of Model Validity

Through analysis of desirability function, optimal results have been validated by conducting three confirmatory tests. The process parameters and corresponding ferrite content have been selected randomly from Table 6. Table 7 displays the tested results at optimum condition. It is revealed from Table 7 that there is a small error ratio between predicted and the experimental values, which validates the applied optimization research. The error percentage in this table was calculated as follows:

$$\text{error\%} = \frac{\text{observed values} - \text{predicted values}}{\text{predicted values}}. \quad (3)$$

Figure 5 shows the SEM micrographs of the validation samples. The micrographs also prove that the ferrite content is very close to the ideal value (50% ferrite) and no detrimental intermetallic phases appear in it.

6. Conclusions

The influence of flux-cored arc welding parameters (welding current, welding voltage, welding speed, and torch angle with reference to vertical) on the ferrite content for 2205 DSS welds has been studied, and the following conclusions are drawn.

A relationship model was developed to predict the ferrite content of weld metal by using the Taguchi design method. Welding current, welding voltage, welding speed, torch angle with reference to vertical, and the interaction of welding voltage and welding speed are the significant terms for the model. Welding voltage and torch angle with reference to vertical have a negative effect on the ferrite content, while the welding speed and welding current have a positive effect on it. The developed model can be successfully used

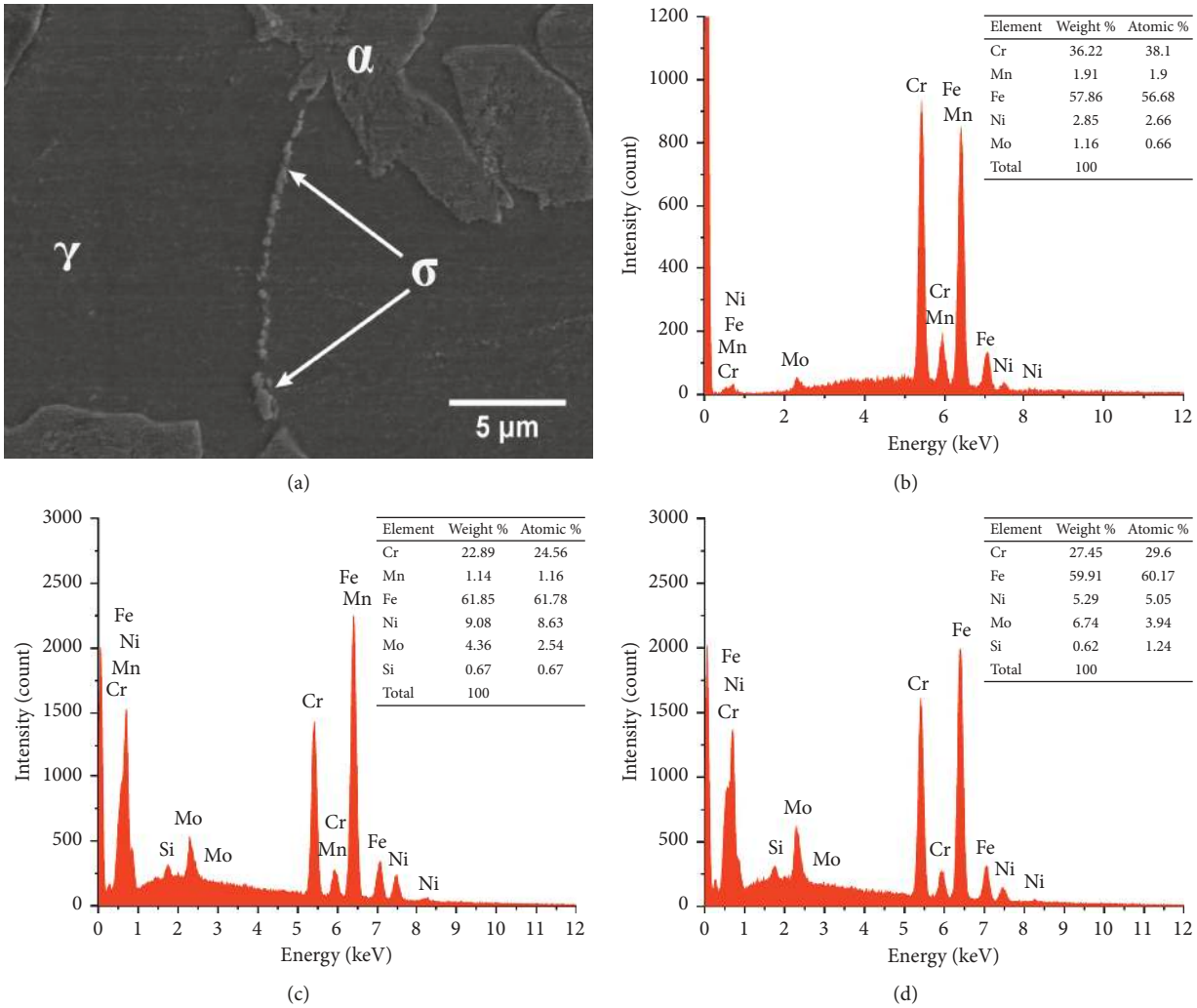

Figure 4: (a) SEM micrograph from 2205 DSS sample welded at trial no. 9 ($I = 240$ A, $U = 26$ V, $S = 22$ cm/min, and $T = 0$ degree); (b) EDS of σ phase corresponding to (a); (c) EDS of austenite phase corresponding to (a); and (d) EDS of ferrite phase corresponding to (a).

Table 5: Process parameter and response constraint.

Parameter or response	Limit		Goals	Importance
	Lower	Upper		3
Welding current	160	240	Is in range	3
Welding voltage	20	26	Is in range	3
Welding speed	18	26	Is in range	3
Welding torch angle with reference to vertical	0	30	Is in range	3
Ferrite content	31.3	51.3	Is target = 50	3

Table 6: Desirable solutions.

Number	I (A)	U (V)	S (cm/min)	T (degree)	Ferrite content	Desirability
1	161.97	21.81	22.94	17.96	49.9999	1.000
2	185.79	20.25	25.55	7.37	50.0001	1.000
3	196.95	20.63	25.70	21.17	50	1.000
4	160.82	20.06	20.47	19.71	50	1.000
5	171.10	20.71	21.84	26.51	49.9999	1.000
6	174.18	20.74	22.34	25.93	50.0001	1.000
7	185.80	20.07	22.68	29.02	50.0001	1.000
8	174.37	20.32	22.32	22.17	50	1.000
9	161.08	25.98	25.28	29.58	49.9999	1.000
10	163.85	20.09	19.71	29.49	49.9999	1.000

Table 7: Validation test results.

Number	Parameters				Ferrite content		Error (%)
	I (A)	U (V)	V (cm/min)	T (degree)	Predicted	Observed	
1	161.97	21.81	22.94	17.96	49.9999	49.6	−0.8
2	185.79	20.25	25.55	7.37	50.0001	49.4	−1.2
3	196.95	20.63	25.70	21.17	50	50.6	1.2

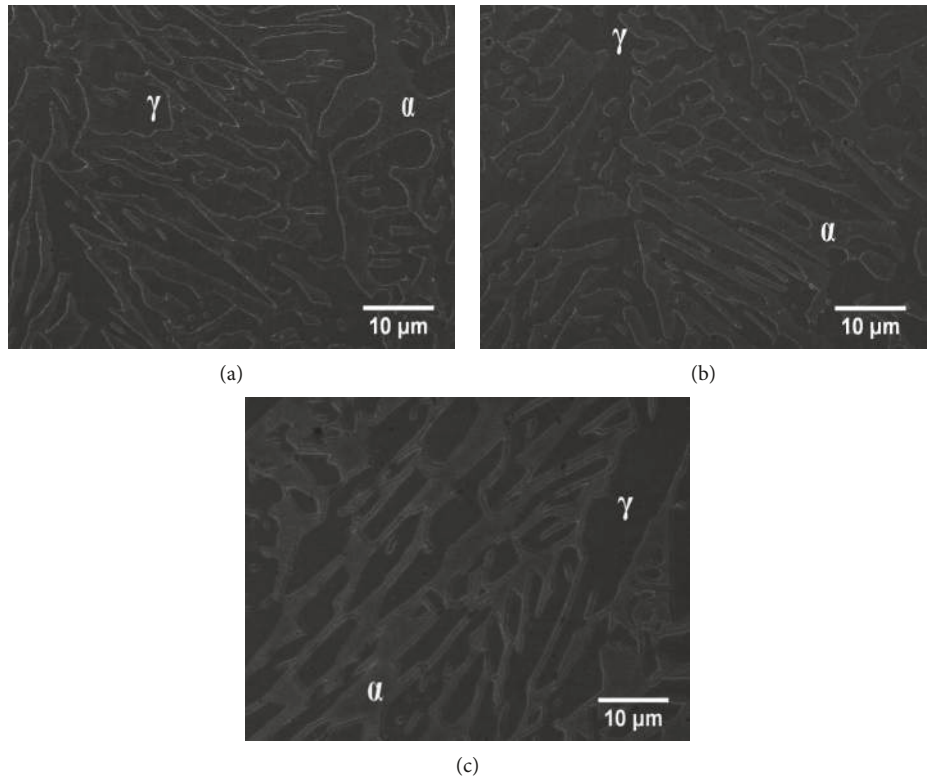

Figure 5: SEM micrographs of the validation samples.

to predict the ferrite content at 95% confidence level and verified by F-test by using the ANOVA table.

To verify the predicted results, three confirmation tests have been implemented, and in the results, errors have been found less than 2%. The results indicate that the developed methods can accurately determine welding parameters so that the desired ferrite content for 2205 DSS welds is achieved.

Data Availability

In the paper, all of the data is available. The data from Table 1 were measured by X-ray fluorescence. In Table 2, the welding parameters are given. For the data from Tables 3–7 and Figures 2 and 3, the optimization process is showed by using the Design-Expert software, and the average ferrite content was measured by the FERITSCOPE MP30.

Conflicts of Interest

The authors declare that they have no conflicts of interest.

Acknowledgments

This work was financially supported by the Foundation of Liaoning Educational Committee (L2017LFW014).

References

[1] R. N. Gunn, *Duplex Stainless Steels: Microstructure, Properties and Applications*, Abington Publishing, Cambridge, England, 1997.

[2] D. H. Kang and H. W. Lee, "Study of the correlation between pitting corrosion and the component ratio of the dual phase in duplex stainless steel welds," *Corrosion Science*, vol. 74, pp. 396–407, 2013.

[3] H.-J. Kim, S.-H. Jeon, S.-T. Kim et al., "Investigation of the sensitization and intergranular corrosion of tube-to-tubesheet welds of hyper duplex stainless steel using an electrochemical reactivation method," *Corrosion Science*, vol. 87, pp. 60–70, 2014.

[4] A.-H. I. Mourad, A. Khourshid, and T. Sharef, "Gas tungsten arc and laser beam welding processes effects on duplex stainless steel 2205 properties," *Materials Science and Engineering: A*, vol. 549, pp. 105–113, 2012.

[5] J. Luo, Y. Yuan, X. Wang, and Z. Yao, "Double-sided single-pass Submerged Arc welding for 2205 duplex stainless steel," *Journal of Materials Engineering and Performance*, vol. 22, no. 9, pp. 2477–2486, 2013.

[6] S. Wang, Q. Ma, and Y. Li, "Characterization of microstructure, mechanical properties and corrosion resistance of dissimilar welded joint between 2205 duplex stainless steel and 16MnR," *Materials and Design*, vol. 32, no. 2, pp. 831–837, 2011.

[7] Y. S. Sato and H. Kokawa, "Preferential precipitation site of sigma phase in duplex stainless steel weld metal," *Scripta Materialia*, vol. 40, no. 6, pp. 659–663, 1999.

[8] E. Ozbay, A. Oztas, A. Baykasoglu, and H. Ozbebek, "Investigating mix proportions of high strength self compacting concrete by using Taguchi method," *Construction and Building Materials*, vol. 23, no. 2, pp. 694–702, 2009.

[9] M. Sarıkaya and A. Güllü, "Multi-response optimization of minimum quantity lubrication parameters using Taguchi-based grey relational analysis in turning of difficult-to-cut alloy Haynes 25," *Journal of Cleaner Production*, vol. 91, pp. 347–357, 2015.

[10] M. Pervez, F. Shafiq, Z. Sarwar, M. Jilani, and Y. Cai, "Multi-response optimization of resin finishing by using a Taguchi-based grey relational analysis," *Materials*, vol. 11, no. 3, p. 426, 2018.

[11] M. Yousefieh, M. Shamanian, and A. R. Arghavan, "Analysis of design of experiments methodology for optimization of pulsed current GTAW process parameters for ultimate tensile strength of UNS S32760 welds," *Metallography, Microstructure, and Analysis*, vol. 1, no. 2, pp. 85–91, 2012.

[12] S. Datta, A. Bandyopadhyay, and P. K. Pal, "Grey-based Taguchi method for optimization of bead geometry in submerged arc bead-on-plate welding," *International Journal of Advanced Manufacturing Technology*, vol. 39, pp. 1136–1143, 2008.

[13] N. Ghosh, P. K. Pal, and G. Nandi, "Parametric optimization of MIG welding on 316L austenitic stainless steel by grey-based Taguchi method," *Procedia Technology*, vol. 25, pp. 1038–1048, 2016.

[14] C. Schneider, C. Lisboa, R. Silva, and R. Lermen, "Optimizing the parameters of TIG-MIG/MAG hybrid welding on the geometry of bead welding using the Taguchi method," *Journal of Manufacturing and Materials Processing*, vol. 1, no. 2, p. 14, 2017.

[15] J. Joseph and S. Muthukumaran, "Optimization of pulsed current GTAW process parameters for sintered hot forged AISI 4135 P/M steel welds by simulated annealing and genetic algorithm," *Journal of Mechanical Science and Technology*, vol. 30, no. 1, pp. 145–155, 2016.

[16] N. Kumar, M. Mukherjee, and A. Bandyopadhyay, "Comparative study of pulsed Nd:YAG laser welding of AISI 304 and AISI 316 stainless steels," *Optics and Laser Technology*, vol. 88, pp. 24–39, 2017.

[17] G. Longlong, Z. Hualin, L. Shaohu, L. Yueqin, X. Xiaodong, and F. Chunyu, "Formation quality optimization and corrosion performance of inconel 625 weld overlay using hot wire pulsed TIG," *Rare Metal Materials and Engineering*, vol. 45, no. 9, pp. 2219–2226, 2016.

[18] R. Lokesh, V. S. Senthil Kumar, C. Rathinasuriyan, and R. Sankar, "Optimization of process parameters tool pin profile, rotational speed and welding speed for submerged friction stir welding of AA6063 alloy," *International Journal of Technical and Research Applications*, vol. 12, pp. 35–38, 2015.

[19] S. C. Juang and Y. S. Tarng, "Process parameter selection for optimizing the weld pool geometry in the tungsten inert gas welding of stainless steel," *Journal of Materials Processing Technology*, vol. 160, pp. 128–137, 2005.

[20] H. Tebassi, M. A. Yallese, I. Meddour, F. Girardin, and T. Mabrouki, "On the modeling of surface roughness and cutting force when turning of Inconel 718 using artificial neural network and response surface methodology: accuracy and benefit," *Periodica Polytechnica Mechanical Engineering*, vol. 61, no. 1, pp. 1–11, 2017.

[21] J. D. Kordatos, G. Fourlaris, and G. Papadimitriou, "The effect of cooling rate on the mechanical and corrosion properties of SAF 2205 (UNS 31803) duplex stainless steel welds," *Scripta Materialia*, vol. 44, no. 3, pp. 401–408, 2001.

[22] C. T. Kwok, S. L. Fong, F. T. Cheng, and H. C. Man, "Pitting and galvanic corrosion behavior of laser-welded stainless steels," *Journal of Materials Processing Technology*, vol. 176, no. 1–3, pp. 168–178, 2006.

[23] J. H. Potgieter, P. A. Olubambi, L. Cornish, C. N. Machio, and El-S. M. Sherif, "Influence of nickel additions on the corrosion behaviour of low nitrogen 22% Cr series duplex stainless steels," *Corrosion Science*, vol. 50, no. 9, pp. 2572–2579, 2008.

[24] E. Taban and E. Kaluc, "Welding behaviour of duplex and superduplex stainless steels using laser and plasma ARC welding processes," *Welding in the World*, vol. 55, no. 7-8, pp. 48–57, 2013.

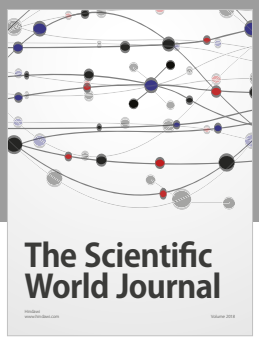

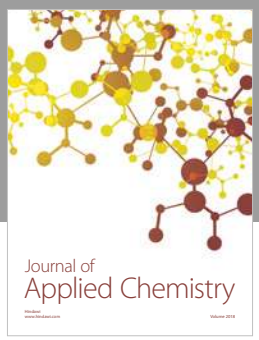

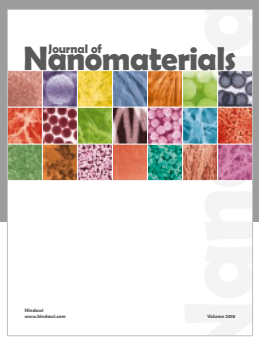

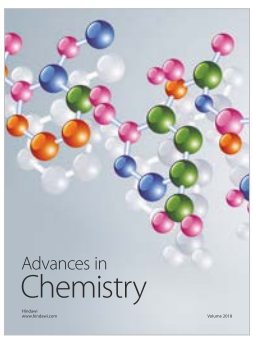

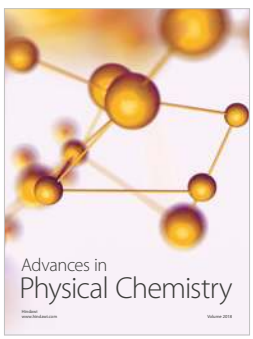

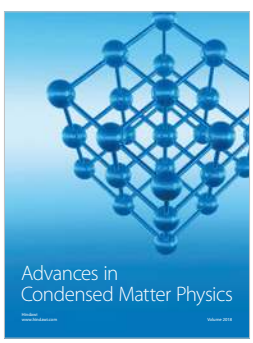

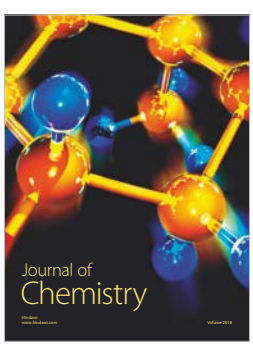

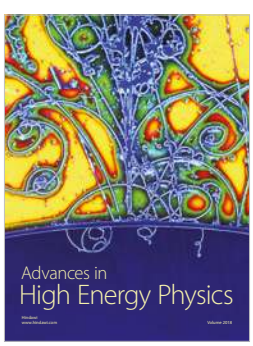

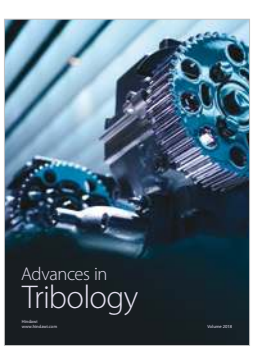

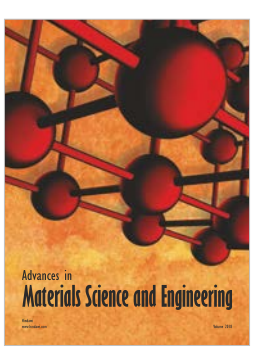

Hindawi

Submit your manuscripts at
www.hindawi.com